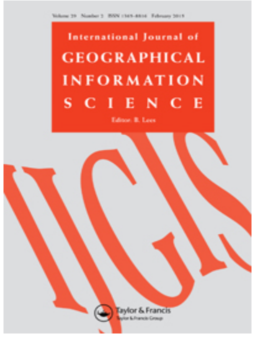

Taylor & Francis
Taylor & Francis Group

International Journal of Geographical Information Science

ISSN: 1365-8816 (Print) 1362-3087 (Online) Journal homepage: https://www.tandfonline.com/loi/tgis20

Using geographically weighted regression kriging for crop yield mapping in West Africa

Muhammad Imran, Alfred Stein & Raul Zurita-Milla

International Journal of Geographical Information Science, 2015
Vol. 29, No. 2, 234–257, http://dx.doi.org/10.1080/13658816.2014.959522

Taylor & Francis
Taylor & Francis Group

Using geographically weighted regression kriging for crop yield mapping in West Africa

Muhammad Imran*, Alfred Stein and Raul Zurita-Milla

Faculty of Geo-Information Science and Earth Observation (ITC), University of Twente, The Netherlands

(*Received 14 July 2012; final version received 20 August 2014*)

Geographical information systems support the application of statistical techniques to map spatially referenced crop data. To do this in the optimal way, errors and uncertainties have to be minimized that are often associated with operations on the data. This paper applies a spatial statistical approach to upscale crop yields from the field level toward the scale of Burkina Faso. Observed yields were related to the Normalized Difference Vegetation Index derived from SPOT-VEGETATION. The objective was to quantify the uncertainties at the subsequent steps. First, we applied a point pattern analysis to examine uncertainties due to the sampling network of field surveys in the country. Second, geographically weighted regression kriging (GWRK) was applied to upscale the yield observations and to quantify the corresponding uncertainty. The proposed method was demonstrated with the mapping of sorghum yields in Burkina Faso and results were compared with those from regression kriging (RK) and kriging with external drift using a local kriging neighborhood (KEDLN). The proposed method was validated with independent yield observations obtained from field surveys. We observed that the lower uncertainty range value increased by 39%, and the upper uncertainty range value decreased by 51%, when comparing GWRK with RK and KEDLN. Moreover, GWRK reduced the prediction error variance as compared to RK (20 vs. 31) and to KEDLN (20 vs. 39). We found that climate and topography had a major impact on the country's sorghum yields. Further, the financial ability of farmers influenced the crop management and, thus, the sorghum crop yields. We concluded that GWRK effectively utilized information present in the covariate datasets and improved the accuracies of both the regional-scale mapping of sorghum yields and was able to quantify the associated uncertainty.

Keywords: regional crop yields; GWR; sorghum; accuracy and uncertainty

1. Introduction

Sustainable farming strategies aim at yield levels while protecting the environment. To accomplish this, bio-economic farm models (BEFMs) were developed (van Ittersum *et al.* 2008). BEFMs can optimize agricultural farm responses by simultaneously assessing the plethora of factors of sustainable farming and the resulting trade-offs among the bio-physical, economic, and socioeconomic goals. Commonly, BEFMs are used as a site-specific application on which all input datasets have been prepared beforehand for a particular farm or village. This contrasts a wall-to-wall application, for which no specific site has yet been identified, and where the model is applied to any site in subregions of a large region. Providing crop yield estimates for wall-to-wall applications is challenging, as it requires timely and accurate mapping of crop yields over large areas, considering local

*Email: imran@pucit.edu.pk

factors of crop yields (Vossen 1999). Crop models and GIS databases are indispensable to map crop yields at national and regional scales. For this, often empirical models are used with low input data requirements, thus avoiding site specificity (de Wit *et al.* 2008). GIS databases developed from national surveys and other global datasets allow deriving external covariates that determine location-specific factors of crop yields. The accuracy of the empirical relations and of the covariates leverages the accuracy of crop yield mapping and, thus, increases the efficiency of wall-to-wall applications. Analyzing, quantifying, and reducing the uncertainties, however, have so far received little attention when developing empirical models of crop yield prediction.

Uncertainty in prediction models is hardly avoidable because the prediction at an unsampled location is always associated with error. Specifically in crop yield mapping, environmental and management factors make yield highly variable in space. Failure to incorporate such high spatial variability contributes to the uncertainty ranges of crop yield models. Recent studies highlighted huge inaccuracies in yield assessments, when crop models were applied at the national and regional scales (Reidsma *et al.* 2009, Challinor *et al.* 2009). These inaccuracies primarily resulted from the inability of the models to utilize information present in environmental and management datasets. Other studies observed that such inaccuracies resulted not only from the quality of the models itself, but also from the quality of acquisition methods of the input covariate datasets (Faivre *et al.* 2004). Moreover, completely ignoring the external covariates that determine spatial variability of crop yields has been considered a major reason of unsatisfactory performance of crop models at regional scales (Reidsma *et al.* 2007). This is particularly true in data scarce regions where limitations in data and even the quality of available data make the quantitative assessment of the models difficult.

Geostatistical models have inherent procedures to deal with uncertainties (Castoldi *et al.* 2009). Kriging, for instance, predicts a target variable by taking into account the spatial dependence between data, and the kriged estimate at each unsampled location includes the standard deviation of the prediction error. Ordinary kriging (OK) considers the spatial configuration of observed data. Moreover, co-kriging and regression kriging (RK) provide ways to incorporate the variability in the external covariate datasets into the kriged predictions (Papritz and Stein 1999). RK allows the variance to vary in space by fitting a trend for the external covariate datasets with MLR (Diggle *et al.* 1998).

For large regional areas, however, global variograms may not incorporate effectively the spatial variability. To deal with this, the nonstationary kriging methods stratify the space and use local variogram models for each stratum (Harris *et al.* 2010b, Lloyd 2011). Spatial regression methods like geographically weighted regression (GWR) use kernel functions to weigh both observations and covariate datasets directly at each calibration point (Brunsdon *et al.* 1996, Fotheringham *et al.* 2002). Here we use a novel approach for crop yield modeling that applies GWR in combination with RK (Harris *et al.* 2010a, Harris and Juggins 2011, Lloyd 2011). Such a hybrid GWRK predicts an attribute at unsampled locations by modeling the locally varying trend using external covariates of observed attribute. To model uncertainty, it then applies kriging to regression residuals.

The study focuses on yield mapping in West Africa where sorghum and millet comprise the staple cereal of people living in this drought-prone region (Maunder 2002). In Burkina Faso, sorghum is the major cereal for food consumption, that is, 34% of all cereals (FAO 1998). The Famine Early Warning System Network (FEWSNET 2012) monitors yields of cereal crops countrywide, including sorghum to mitigate food crises.

The main objective of this study is to predict sorghum crop yield and its uncertainty at a regional scale in West African cropping system, using the crop yield observations obtained from countrywide georeferenced surveys. The study was applied to Burkina Faso that has relatively high spatial variability of sorghum crop yields due to strong variation of the environment conditions. Here, we first investigated the sampling network of field surveys. Next, we explored GWRK for prediction and associated measures of prediction uncertainty, and compared it with other geostatistical methods.

2. Materials and methods

2.1. Study area

Burkina Faso has dominant rainfed agriculture. Spatial variability of climate in the country is characterized by a strong north–south annual rainfall gradient. The average annual rainfall decreases 1 mm per km and, besides this latitudinal trend, a difference of 200–300 mm may occur in any direction within a radius of only 100 km (Graef and Haigis 2001). Rain falls during the 3–5 summer months, with half of the rainy days occurring in July and August (Graef and Haigis 2001). Crops are grown during the rainy season. Periodic droughts and strong spatial rainfall and land variability restrain the farmers to adapt agricultural management strategies at the local level than at the national level (West *et al.* 2008). The farmers apply these strategies commonly on their individual farm lands in a farmer's community, the so-called terroirs. A terroir is the basic unit of communal agricultural management. It is led by a traditional chief. The next administrative level is the district. Conventional subsistence or small-scale farming is the mainstay agricultural activity in Burkina Faso, covering approximately 85% of cultivated lands (UNCCD 2000). This type of farming is typically associated with a low level of inputs, low financial ability of farmers, manual labor, local cultivars, little or no fertilization, no crop protection, and small-area farms run by households and having less accessibility to markets. Sorghum is typically grown in subsistence farming.

2.2. Crop yield sampling and analysis

Crop yield data were collected from the Statistiques Agricoles (AGRISTAT) Burkina Faso (AGRISTAT 2010). AGRISTAT compiles household survey data for representative terroirs in order to reduce the operational costs. AGRISTAT measures the areas and the geographical locations of the household parcels, and gets the weight (kg) of the sorghum grains from all those measured parcels in a representative terroir. In this study, the AGRISTAT (georeferenced) household surveys for the year 2009 were used to obtain observed sorghum crop yield (kg ha^{-1}) per representative terroir, providing a total of 280 observations in the country.

Inadequacy in the configuration of observation sites contributes to erroneous assessment of the relations between observations and external covariate datasets (Challinor *et al.* 2009). A factor that may contribute to this uncertainty is the spatial clustering of observation sites. It is usually assumed that the representative terroir locations are not significantly clustered. This assumption was tested from theoretical backgrounds of the point pattern analysis (Cressie 1993). The geo-referenced locations of the representative terroirs presented in Figure 1a were considered as the 'points'. The bounding shape for the point pattern was a mask of the study area, that is, the validity domain (Kanevski 2008). The Ripleys K-function was used as a statistical measure, to calculate the degree of spatial randomness in the spatial distribution of crop yield samples (Ripley 1988), following the procedures implemented by Baddeley and Turner (2005). Edge correction was applied

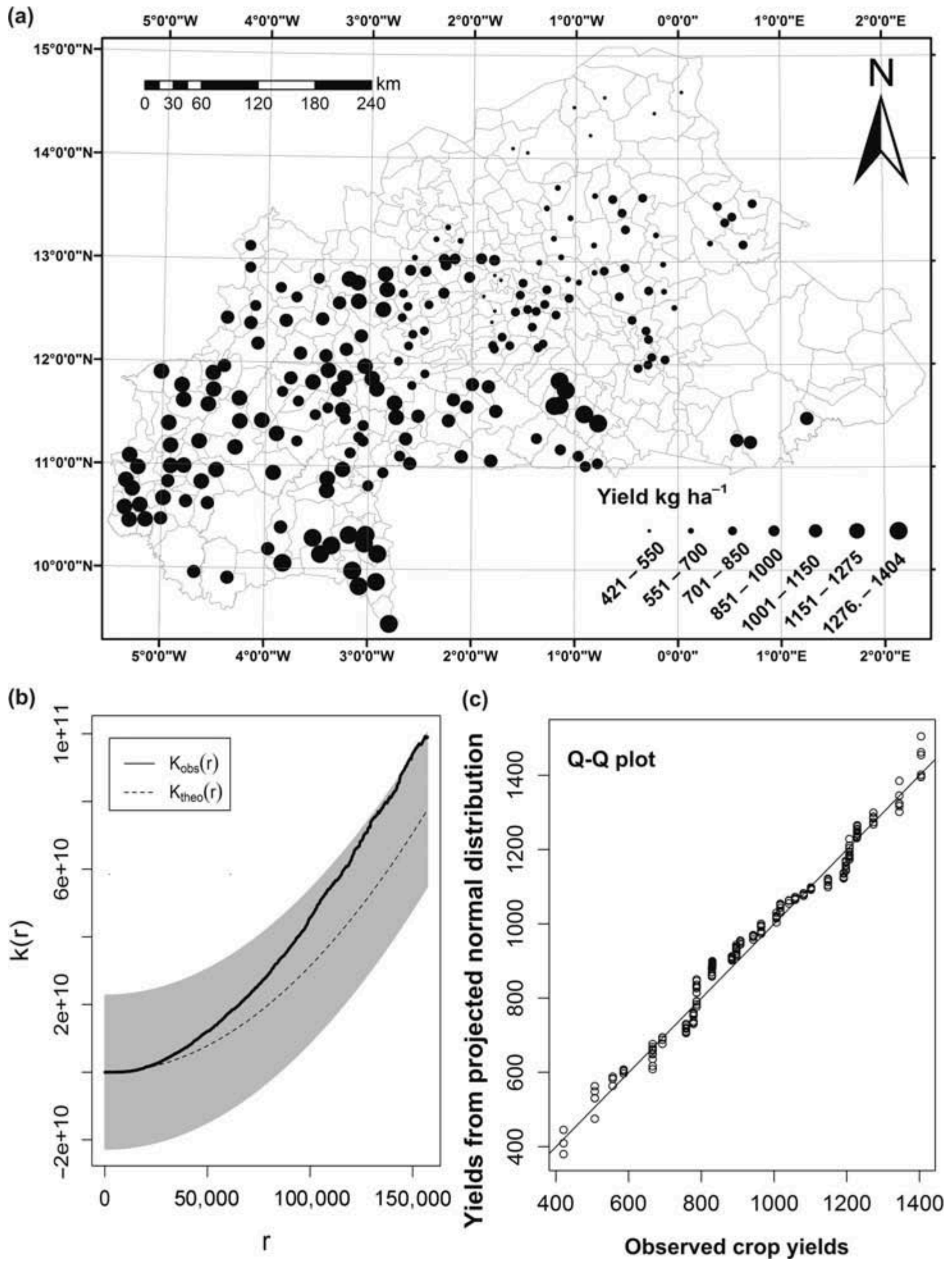

Figure 1. Observed sorghum yield (kg ha^{-1}) for year 2009 in the study area (a), K-function for observation sites plotted together with the envelope of the *K*-function (gray) for 100 simulated random patterns. Black solid line shows the estimated *K*-values of the observation sites for different distances. This line lies inside the envelope and confirms that the pattern of observation sites is random (b), Q-Q plot comparing the observed sorghum yield (horizontal axis) to the yields form projected normal distribution with the standard deviation and mean values of observed sorghum crop yield (vertical axis) (c).

using the border method (Ripley 1988). Simultaneous envelopes under complete spatial randomness were computed based on 100 simulations of random distributed points over the study area. The test rejects the null hypothesis if the graph of the K-function for the sampled points lies outside the envelope at any distance. Regression models in this study assume that independent data satisfy i.i.d. assumptions, that is, the data follow the normal distribution and have a constant variance. A Kolmogorov–Smirnov (K–S) two-side test was used to test normality of data.

2.3. Preparing external covariates of crop yield

Crop yields are primarily influenced by local climate, land characteristics, and the levels of inputs and management applied to the land. The following external covariate datasets were used to model the sorghum crop yield: remote sensed-based vegetation indices, rainfall, topography, rural population density (RURP), poverty head count ratio (PHCR), and market access.

The Normalized Difference Vegetation Index (NDVI) is a RS-based vegetation index, calculated as: $NDVI = (NIR - R)/(NIR + R)$, where NIR is the spectral reflectance in the near-infrared where top-of-the-canopy reflectance is dominant, and R is the reflectance in the red portion of the spectrum where chlorophyll absorbs strongly (Dorigo *et al.* 2007). The NDVI was used as a biophysical indicator of the vegetation productivity during the sorghum growing season. NDVI data were obtained from the SPOT-VEGETATION sensor. We used a georeferenced temporal series of 10-day NDVI composites with a spatial resolution of 1 km^2. These products are a combination of daily atmospherically corrected data of all vegetation measurements of the given decade into a single image, using the maximum value composite algorithm. In total, 18 images were obtained for the sorghum growing season from June 2009 to November 2009. Principal component analysis (PCA) was performed to obtain the standardized principal components of NDVI (NDVI.PCs), to reduce the dimensionality of data and to remove multicollinearity.

Climatic conditions are important determining factors for sorghum crop yield (Graef and Haigis 2001). The Tropical Applications of Meteorology using Satellite (TAMSAT) merges the satellite data with rain gauges observations to derive rainfall estimates (0.0375°≈ 4 km spatial resolution) over the African region (Grimes *et al.* 1999). We obtained 10-day TAMSAT rainfall data for the year 2009. For scale adjustment, the TAMSAT data were resampled to 1 km^2 using bilinear interpolation. To reduce the data dimensionality, PCA was performed to obtain the principal components of rainfall time series (PREC.PCs).

Topography affects the crop performance, in both low and high rainfall conditions (West *et al.* 2008). For instance, central and northern Sahelian farmers mostly abandon the marginal uplands and elevated borders of lowland fields because those land types perform poorly in low rainfall conditions. Similarly, in the regions of higher rainfall conditions toward southern Burkina Faso, the lowland fields are prone to get flooded, due to runoff to/from neighboring lands. Elevation was selected as a topographical variable. Elevation data (ELEV) were obtained from Hydro 1-km Africa datasets (USGS 2012).

Extensive data on characteristics of individual farms are used to relate location-specific management data and crop yields. For instance, Reidsma *et al.* (2007) using the Farm Accountancy Data Network data observed that levels of inputs and capital intensity of farmers influenced wheat yields at the European scale. Such extensive data were not available in Burkina Faso. To access management applied to terroirs, we therefore used regional grids of socioeconomic data as proxy indicators, which are explained below.

Financial ability of farmers influences input intensity, for example, fertilization use, pest control use, and use of improved crop cultivars. In subsistence farming, the levels of inputs may be marginalized depending on where the population is living. In areas where a larger population is living below poverty, farmers may have less capital to invest in improved levels of inputs. A commonly used metric is the PHCR, being the percentage of the population living below the established poverty line. We used the 1.25 poverty line, that is, less than 1.25 US dollar purchasing power parity (PPP) per day. For this, the gridded data of sub-national PHCR (1 km^2) were obtained from (HarvestChoice 2012), expressed in 2005 international equivalent PPP dollars.

Availability of labor in a terroir is a crop management factor in subsistence farming. Depending on labor availability, the farmers use intensive land management to increase yields per hectare of cropped area (West *et al.* 2008). We used RURP as proxy for labor availability. The RURP, that is, the number of rural people per km^2 (2005), was obtained from HarvestChoice (2012).

Accessibility to markets is a reliable estimator of crop areas at a regional scale (Ramankutty 2004). Crop areas can be used as proxy to determine capital intensity of farms (Reidsma *et al.* 2007). Low capital intensity prohibits farmers of remote terroirs to transport their crops to the market or modern inputs back to their farms (Fortanier 2006). Larger crop areas were expected closer to markets, having more capital available for investments in new technologies. Market access (MARK) was calculated based on the map of major markets of Burkina Faso, obtained from FEWSNET (2012). A simple model was applied based on the distance of a terroir to its nearest markets. The obtained gridded dataset has a cell size equal to 1 km^2.

2.4. Statistical analysis

The first step in the statistical analysis is the definition of a regularly spaced grid covering the study area with a cell size equal to 1 km^2. We define our spatial model to predict crop yield at visited and unvisited grid cells using the values of the covariates, as

$$\begin{aligned} Y(s) = f(&NDVI.PC(s), PERC(s), ELEV(s), RURP(s), PHCR(s), MARK(s)) \\ &+ H(s), \end{aligned} \tag{1}$$

where $Y(s)$ represents the sorghum yield at a location s that is modeled in two components: a trend function f and an error model $H(s)$, denoting the small-scale fluctuations around f with variance $VAR\{H(s)\}$. The function f determines the overall influence of the external covariates $NDVI.PC(s)$, $PERC(s)$, $ELEV(s)$, $RURP(s)$, $PHCR(s)$, $MARK(s)$, following the notations in the previous section. It was modeled as a global linear function using MLR when applying RK, and as a local linear function using GWR when applying GWRK, respectively.

2.4.1. MLR and GWR

MLR and GWR were applied to model the sorghum yield trend. The coefficients of these regression models were applied to predict the yield at unvisited locations using the grid cell values of the external covariates at those locations.

MLR assumes that $H(s)$ is a stationary random field with $E\{H(s)\} = 0$ and $VAR\{H(s)\} = G$, where the elements of the $n \times n$ diagonal matrix G reflect a pure nugget variance, that is, zero spatial autocorrelation, with $G = \sigma^2 I$. In the case of MLR, the regression coefficients are estimated as $\hat{\beta}_{MLR} = C_{MLR}Y$, where $C_{MLR} = (X^T X)^{-1} X^T$, and X is the matrix with covariates (Chambers and Hastie 1992). The MLR prediction at s is

$$\hat{Y}_{MLR}(s) = x_{\circ}(s)^T \hat{\beta}_{MLR} \tag{2}$$

where $x_{\circ}(s)$ is a vector of covariates at a grid cell s. The MLR prediction error variance at s is estimated as

$$VAR[\hat{Y}_{MLR}(s) - Y(s)] = [1 + x_{\circ}(s)^T (X^T X)^{-1} x_{\circ}(s)]\hat{\sigma}^2_{MLR}, \tag{3}$$

where $\hat{\sigma}^2_{MLR} = RSS/(n - np)$, RSS is the residual sum of squares, and the denominator term is known as effective degrees of freedom (DF) of the residual, and np is equivalent to the number of parameters in a global linear model.

Similar to MLR, GWR assumes that $H(s)$ is a stationary random field. GWR parameters are estimated locally at all observed locations, as $\hat{\beta}_{GWR}(s) = C_{GWR}Y(s)$, where $C_{GWR} = (X^T W(s) X)^{-1} X^T W(s)$ (Fotheringham *et al.* (2002), pp. 55). Here, $W(s)$ is a $n \times n$ diagonal matrix of spatial weights. The weighting matrix is specified by means of a kernel function. We used a Gaussian function as the kernel function to specify a weighting matrix considering the neighboring terroir locations,

$$W_{st} = exp[-0.5(d_{st}/b)^2], \tag{4}$$

where b is a (non-negative) kernel bandwidth and d_{st} are the distances between s and neighboring terroir locations t. The kernel bandwidth measures the distance decay in the kernel function. It was specified as adaptive, that is, a proportion between 0 and 1 of observations to include in the weighting scheme (Bivand *et al.* 2008). Also, spatial scale dependency required confirming the spatial nonstationarity of the relationship between crop yield and its external factors. This required examining the effect of different adaptive bandwidths on local estimation in GWR and finding an optimal kernel bandwidth. To do so, we minimized Akaike's information criterion (AIC) (Fotheringham *et al.* (2002), pp. 212) and increased the GWR adaptive bandwidth measures in small steps ($0.05 = 10N_t$, $0.1 = 20N_t$, $0.15 = 30N_t$, $0.2 = 40N_t$, $0.25 = 50N_t$, and $0.3 = 60N_t$, where N_t is the number of neighboring terroirs). For each step, we recorded the value of the spatial stationarity index (Fotheringham *et al.* 2002, Gao *et al.* 2012), which is a ratio between the interquartile range for the GWR coefficients and twice the standard error (SE) of the same variables from the equivalent global model.

The local relations estimated by GWR were then used to predict the crop yield at unvisited locations as

$$\hat{Y}_{GWR}(s) = x_{\circ}(s)^T \hat{\beta}_{GWR}(s), \tag{5}$$

with the GWR prediction error variance at s (Leung *et al.* 2000) as,

$$VAR[\hat{Y}_{GWR}(s) - Y(s)] = [1 + x_{\circ}(s)^T (C_{GWR} C^T_{GWR}) x_{\circ}(s)]\hat{\sigma}^2_{GWR}, \tag{6}$$

where $\hat{\sigma}^2_{GWR} = RSS/(n - np)$, here the term np can be denoted as the effective number of parameters for the GWR model.

2.4.2. OK and KED

OK allows predicting a spatially dependent attribute, using a variogram that relates the autocorrelation to the separation distance between two sample locations. OK was used to interpolate observed crop yields and also the residuals from MLR and GWR. The OK kriging predicts crop yield at an unvisited location s (Cressie (1993), p. 119) as

$$\hat{Y}(s) = \sum_{s=1}^{n} W_s.Y(s_i), \sum_{s=1}^{n} W_s = 1 \tag{7}$$

Here, W_s is the weight assigned to each of the observed crop yields and it is yet unknown. The condition that the sum of weights is equal to 1 makes the $VAR[\hat{Y}_{OK}(s) - Y(s)]$ minimal among all linear unbiased predictors.

When applying OK, we write $VAR\{H(s)\} = G'$, where G' is a $n \times n$ matrix, whose elements are found from variogram $\gamma(h)$ and reflect covariances of the sample locations. The variogram model used in this study was the exponential model:

$$\gamma(h) = \left\{ \begin{array}{ll} 0 & \text{if } h = 0 \\ C_0 + C_1.[1 - exp\left(\frac{-h}{a}\right)] & \text{if } 0 \le h \le a \end{array} \right\} \tag{8}$$

Here, C_0 is small-scale nugget variance, C_1 is a large-scale structural variance, and a is the correlation range. To analyze possible anisotropy in the variogram model, directional variograms were computed for four main directions: 0°, 45°, 90° and 135°. Moreover, the variability of the empirical variogram was analyzed with larger distances (Diggle and Ribeiro 2007). To do so, the isotropic variogram model was fitted using weighted least squares (WLS) and its confidence bands (envelopes) were computed.

The spatial covariances between the values at the prediction and the sample locations are contained in the vector σ'. The unbiased predictor with minimal variance of the prediction error is given by

$$\hat{Y}(s) = x_{\circ}(s)^T \hat{\beta}_{GLS} + \sigma'^T G'^{-1}(Y - X\hat{\beta}_{GLS}), \tag{9}$$

where the trend parameters $\hat{\beta}$ are estimated from generalized least squares (GLS) as, $\hat{\beta}_{GLS} = (X^T G'^{-1} X)^{-1} X^T G'^{-1} Y$. In the case of OK, X consists of a vector with values 1 only, whereas for KED, it extends with an additional column of the values of the external covariates. The prediction error variance for KED is

$$\begin{aligned} VAR\ [\hat{Y}(s) - Y(s)] = \{\hat{\sigma}^2 - \sigma'^T G'^{-1} \sigma'\} + (x_{\circ}(s) - X^T G'^{-1} \sigma')^T . (X^T G'^{-1} X)^{-1} \\ \times (x_{\circ\circ}(s) - X^T G'^{-1} \sigma') \end{aligned} \tag{10}$$

where $\hat{\sigma}^2$ is the estimate of the residual variogram sill $C_0 + C_1$. Again, the OK prediction error variance is obtained on setting a constant trend in Equation (10) (see for details, Papritz and Stein (1999), pp. 95–98).

Here we applied KED with a local kriging neighborhood (KEDLN) through considering local neighborhoods of sample points instead of the global sample. The neighborhoods for KEDLN were found using cross-validation.

2.4.3. RK and GWRK

Explicit solving Equations (9) and (10) results into RK, which combines a separately fitted regression on external covariates with kriging of the regression residuals (Diggle *et al.* 1998). Chilès and Delfiner (1999) and Rivoirard (2002) showed that both KED and RK are mathematically equivalent and give the same predictions and error estimates if a global neighborhood is specified. RK as a variant of explicit kriging, however, allows specifying a local, nonparametric, and nonlinear trend component (Cressie 1993). Here we specified both MLR and GWR, to model a trend in RK and GWRK, respectively. In both cases $VAR\{H(x)\}$ includes the covariance between point pair observations. This allows including nonzero spatial autocorrelation of the regression residuals. The procedure we followed was that first variograms of the regression residuals from MLR and GWR were determined, followed by OK of the regression residuals toward the unvisited grid cells. The interpolated residuals were then added to the respective predicted drift surfaces. The RK prediction was then derived as,

$$\hat{Y}_{RK}(s) = x_\circ(s)^T \hat{\beta}_{MLR}(s) + \hat{H}_{OK}(s), \tag{11}$$

and the GWRK prediction as,

$$\hat{Y}_{GWRK}(s) = x_\circ(s)^T \hat{\beta}_{GWR}(s) + \hat{H}_{OK}(s) \tag{12}$$

In this way, both heteroskedasticity of the external trend using the covariates and spatial dependency of residuals were included and compared. Note that $\hat{Y}_{GWRK}(s) = \hat{Y}_{GWR}(s)$, if the GWR residual variogram is determined as a pure nugget variogram. The additive relationship of predictions from Equations (11) and (12) continues to prediction variances as well. Hence, the MLR prediction variance Equation (3) and the GWR prediction variance Equation (6) were added to the OK prediction error of residuals at s (derived from Equation (10)), respectively, to obtain the RK and GWRK prediction error variances at s.

The problems of multicollinearity may arise when the external covariates are highly correlated, resulting in instable results in the estimated regression coefficients (Wheeler and Tiefelsdorf 2005). Following (Wheeler 2007), the nature of global and local collinearity was investigated using the global and local condition numbers, respectively. As a rule of thumb, condition numbers greater than 30 indicate collinearity problems in the global and local regression fits. A matrix scatterplot was used to analyze correlations between external covariates.

2.5. Validation

The observed crop yields were randomly split into training and validation subsets, containing 75% and 25% of independent observations, respectively. To compare MLR and GWR, we used common accuracy and precision statistics such as the RSS, the SE of the estimate, the AIC, GWR ANOVA test, and Monte Carlo test (Fotheringham *et al.* (2002), pp. 212–216). The ANOVA tests the null hypothesis that GWR model represents no improvement over a global model. The Monte Carlo test tests the significance of the spatial variability in the local parameter estimates.

Cross validation (CV) was used to assess the variogram model, in terms of prediction accuracy and the accuracy of corresponding prediction uncertainty, that is, the kriging variances (Pebesma 2004). Using CV of the kriged residuals, we computed the frequency distribution of the *z*-score defined as the residual divided by kriging SE, the mean error (ME), the mean square normalized error (MSNE), and the root mean square error (RMSE) (Pebesma 2004). The spatial structure of the CV residuals was analyzed. The model prediction accuracy was assessed by comparing model predictions with independent observations using statistical techniques (Leopold *et al.* 2006). To do so, the mean absolute error (MAE) and mean square error (MSE) were used. They were calculated as:

$$MAE = \frac{\sum_{n} |\hat{Y}(s) - \hat{Y}_m(s)|}{n} \tag{13}$$

and

$$MSE = \frac{\sum_{n} (\hat{Y}(s) - \hat{Y}_m(s))^2}{n}, \tag{14}$$

where $\hat{Y}(s)$ are the predicted values, $\hat{Y}_m(s)$ are the mean values and n is the number of grid cells.

The R package spgwr (Bivand *et al.* 2008) was used to perform GWR, and the R package Gstat (Pebesma 2004) to automatically fit the variograms and to perform the kriging of GWR and MLR residuals. Block kriging in Gstat was used to deal with the change of support (Pebesma and Wesseling 1998). Since the trend models are linear, we can use model coefficients derived at the point support for estimating at the block support. Then block predictions and corresponding prediction error variances are not affected by a change of support (Heuvelink and Pebesma 1999, Leopold *et al.* 2006). Here, the block size equals 1 km^2 grid cell, which is equal to the grid cell size of external covariate datasets.

3. Results

3.1. Statistical analysis

Figure 1a shows the spatial distribution of the observed sorghum crop yields. The mean observed sorghum yield (954 kg ha^{-1}) in 2009 is slightly below the 10 years (2000–2009) county average yield (969 kg ha^{-1}). There is a clear north–south trend of sorghum yields across the country. High-yield values occur toward the southern part of Burkina Faso, with a subhumid agroecological gradient. This zone has more favorable cropping conditions as compared to the semiarid and arid zones toward the northern parts of the country.

Figure 1b shows that the *K*-function of the observed points lies inside the envelope for each value of *r*. The test confirms (P = 0.05) that the network of representative terroir locations is homogeneously distributed and, hence, declustering is not required (Kanevski and Maignan 2004). The K–S test ($P = 0.1$) confirms normality assumption of the distribution of observed sorghum crop yield. The Q-Q plot (Figure 1c) shows that the highest yields in the distribution of observed sorghum yield are lower than for the corresponding normal distribution, with the maximum difference equal to 200 kg ha^{-1}. This is typically observed in large-scale agricultural surveys. Here we obtain a high degree

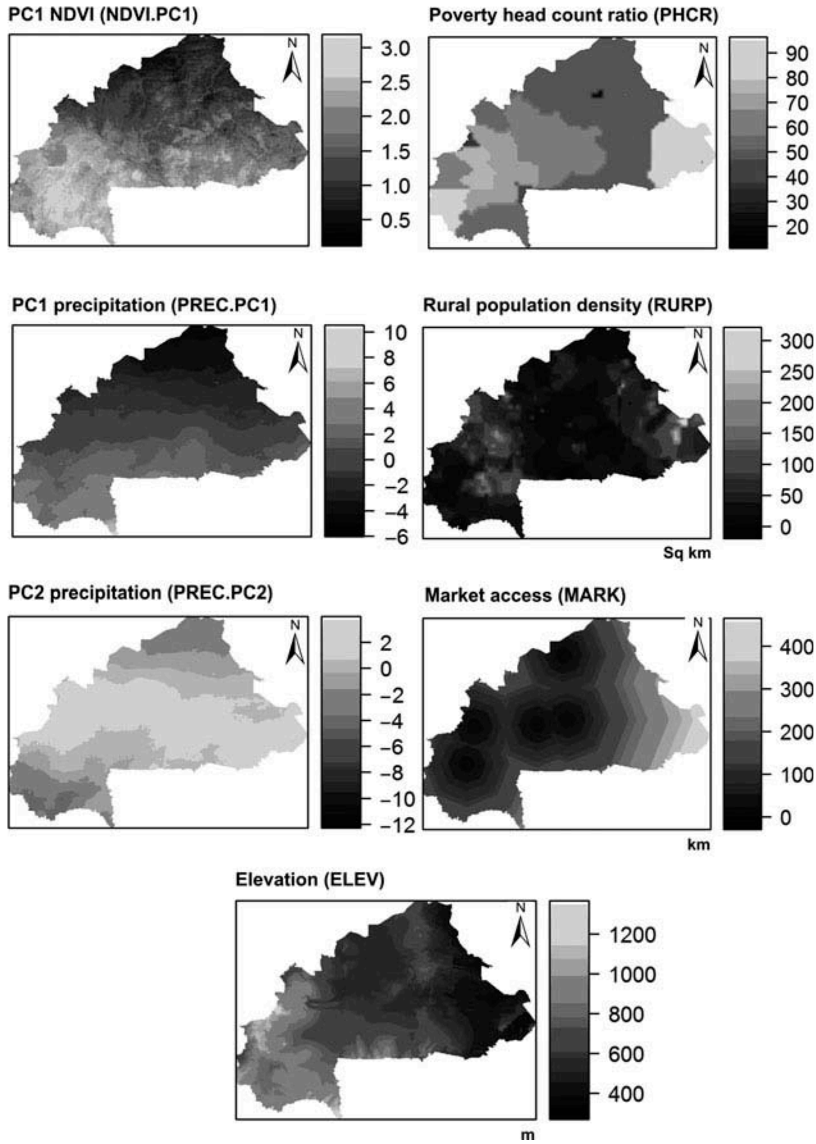

Figure 2. Maps of external covariates to predict sorghum crop yield in Burkina Faso.

of spatially autocorrelation (Moran's $I = 0.81$, $P < 0.001$) of the observed sorghum crop yields.

Figure 2 shows maps of external covariates to predict the sorghum crop yield. PCA of the 10-day SPOT VGT NDVI composite images, covering the sorghum growing season, captures 99% variance of the entire image series into the first three principal components. The first principal component (NDVI.PC1) explains more than 91% of the total variability in the image bands and, therefore, is included in the analysis. Similarly, PCA of the 10-day TAMSAT rainfall estimates allocates approximately 93% of the total variability into the first two principal components (PREC.PC1 and PREC.PC2).

3.2. Regression analysis

Linear regression shows a significant relation ($R_a^2 = 0.64$, $p < 0.001$) between the sorghum yield and those external covariates. The coefficients obtained with MLR are given in Table 1. Since the condition numbers take into account the multivariate predictability of any one covariate from the other covariates, our findings (i.e. condition numbers ≤ 30) show no significant global collinearity. This is further confirmed by the matrix scatterplot (Figure 3a), which shows no bivariate correlations among pairs of selected external covariates. However, the local condition numbers (Figure 4) show a significant collinearity in the local regression fits. A Moran's I value of 0.44 (p < 0.001) for the MLR residuals shows that the model can be improved by (1) using spatial regression methods and (2) kriging of the residuals.

A comparison of the MLR and GWR models is presented in Tables 1 and 2. Minimizing AIC from 2032 to 2016 results in an adaptive bandwidth of 0.05, correspondingly with 6–10 neighboring terroirs. The inter-quartile ranges of the GWR coefficients (Table 1) indicate spatial nonstationarity, that is, the local parameter estimates are highly variable in the study area. The stationarity index becomes larger up to the adaptive bandwidth of 0.05 and flattens with higher bandwidths. For example, the inter-quartile range of NDVI.PC1 in GWR (62.4 to 201) is well beyond the ±1 standard deviation (92.6) of the corresponding MLR estimate. Moreover, at this adaptive bandwidth, a Monte Carlo significance test indicates a significant spatial variation (P = 0.001) in the local parameter estimates for all external covariates. This confirms that the relationship between sorghum yield and external covariates is local and varies in different parts of the study area. For example, Table 1 shows that a significant negative correlation (global) exists between sorghum yield and PREC.PC2 ($r = -0.22$, $P = 0.001$). However, for the same parameter, both the inter-quartile range of the GWR coefficient (−44.50 to 56.00) and the Monte Carlo significance test (P = .001) show that the parameter is spatially nonstationary.

Table 1. Parameter estimates for the sorghum yield model fitted using the multiple linear regression (MLR) and the geographically weighted regression (GWR).

Regression parameters	(r; p)[a]	MLR test[b]	MLR SE[c]	P-value	CN[d]	GWR range[e]	MC test[f]
Intercept	–	135.78	107.52	0.050	1.00	−41.50 to 465.00	0.001
NDVI.PC1	(0.75, <0.0001)	151.39	46.33	0.001	1.93	62.40 to 201.00	0.001
PREC.PC1	(0.73, <0.0001)	31.09	11.47	<0.001	2.92	15.10 to 89.30	0.001
PREC.PC2	(−0.22, 0.001)	40.32	10.77	<0.001	5.71	−44.50 to 56.00	0.001
ELEV	(0.60, <0.0001)	0.32	0.11	<0.001	14.84	−0.23 to 0.37	0.001
PHCR	(0.51, <0.0001)	3.76	1.28	<0.001	18.78	1.46 to 9.27	0.001
MARK	(0.23, 0.001)	0.95	0.31	0.001	23.74	0.73 to 2.58	0.001

Notes: [a]Pearson correlations between the CAI and the variables of the first principal component of Normalized Difference Vegetation Index (NDVI), first two principal components of rainfall estimates (PREC), elevation (ELEV), poverty head count ratio (PHCR) and distance to major trade markets (MARKD).
[b]Parameter estimates from MLR.
[c]Condition numbers.
[d]Standard error.
[e]Inter-quartile range of the GWR coefficients.
[f]Monte Carlo significance test for spatial nonstationarity of parameters.

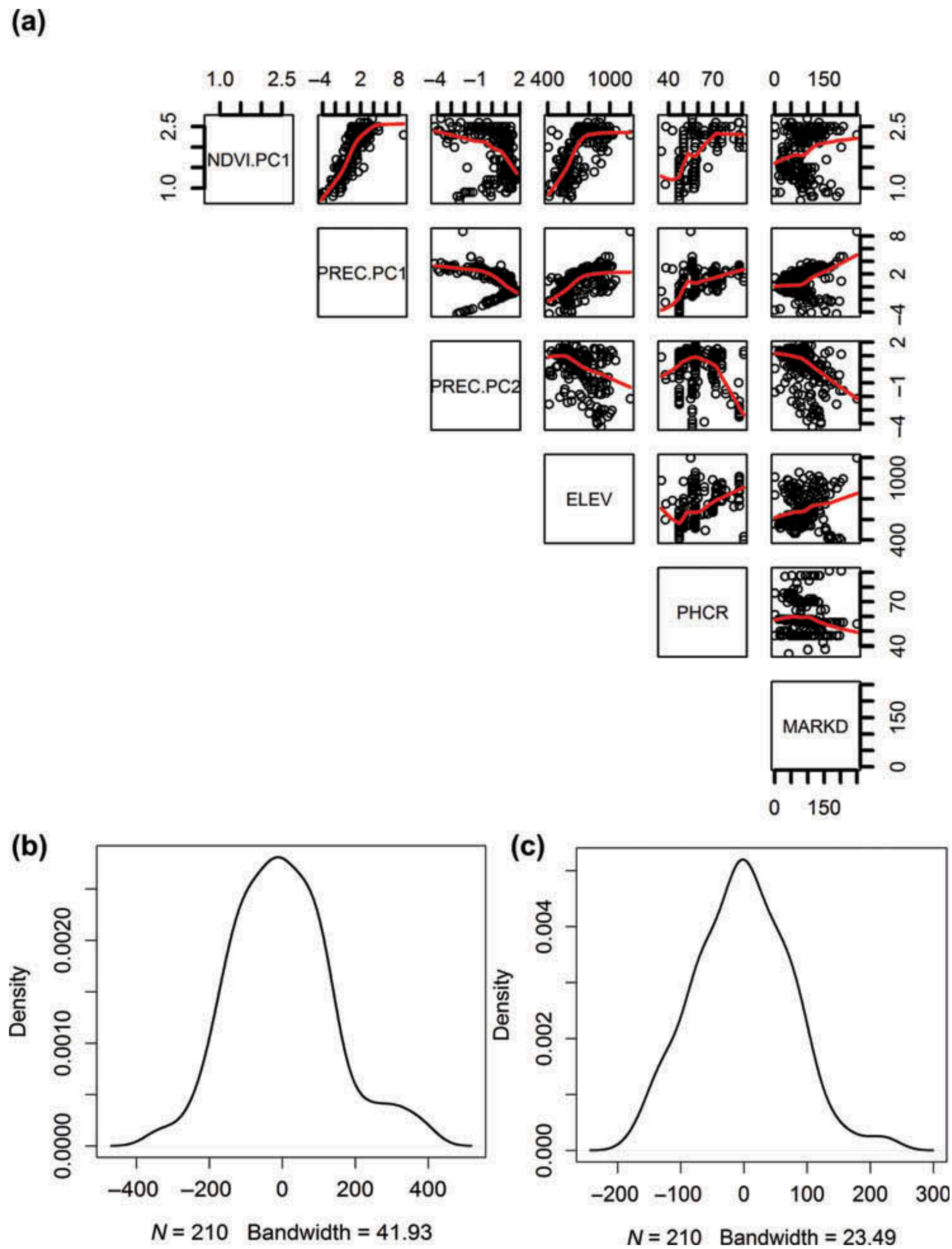

Figure 3. Bivariate correlations between pairs of selected external covariates (a), Kernel density plot of multiple linear regression (MLR) residuals (b), Kernel density plot of geographically weighted regression (GWR) residuals (c).

A low Moran's I value of 0.23 ($P < 0.001$) is observed for the GWR residuals, compared to that of 0.44 ($P < 0.001$) for the MLR residuals. Moreover, the spread of GWR residuals is smaller, as is seen from the density histograms of MLR and GWR residuals in Figure 3b–c. This suggests that GWR accounts for most of the spatial

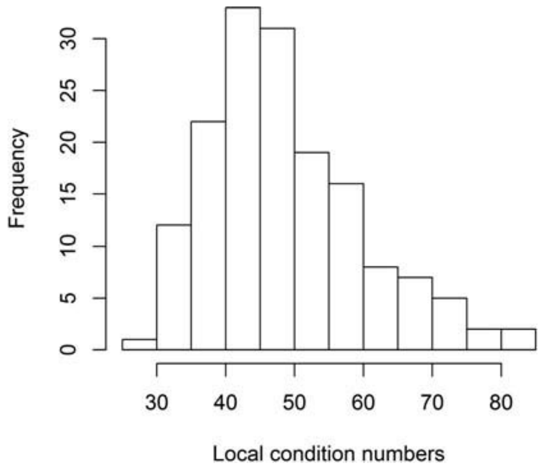

Figure 4. Histogram of the local condition numbers.

Table 2. Accuracy and precision statistics for sorghum regression models fitted using both the global multiple linear regression (MLR) and geographically weighted regression (GWR) approaches.

Model	RSS[a] (sqrt)	SE[b]	DF	F	AIC[c]	R_a^2 [d]
MLR	1790	190	7	–	2032	0.62
GWR	1241	121	105	2.47	2016	0.83

Notes: [a]Residual sum of square.
[b]Standard error.
[c]Akaike information criterion.
[d]Adjusted coefficient of determination.

variability in the sorghum yields from the spatial variability of the external covariate data. Next, spatial structure observed in the GWR and MLR residuals is to be incorporated to construct GWRK and RK models, respectively.

The results of the ANOVA test (Table 2) indicate that the GWR model is a statistically significant ($P < 0.05$) improvement over its corresponding MLR model for the sampled sorghum yield data. The RSS and SE values in the sorghum yield estimations are reduced in the GWR model. The adjusted coefficient of determination, R_a^2, increased from the global MLR to the GWR model, although an increase can be expected relating to the difference in the DF. The reduction in the AIC from the MLR model shows, however, that the GWR approach is better even after considering the differences in DF.

3.3. Geostatistical analysis

Figure 5a shows the standard variograms fitted for sorghum yield in 0°, 45°, 90° and 135° directions. The sill values of these variograms, equal to 50,477 kg^2, 44,196 kg^2, 38,149 kg^2, 47,489 kg^2, respectively, as compared to that of the omnidirectional variogram, equal to 45,517 kg^2, show no anisotropy. Moreover, the fitted isotropic variogram goes through all points and lies within the confidence bands (Figure 5b). The confidence

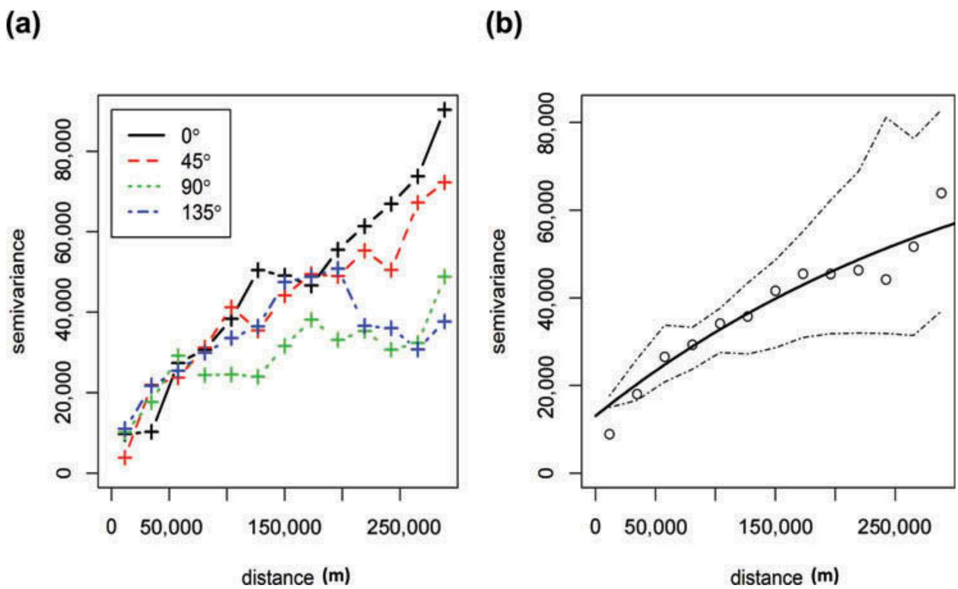

Figure 5. Standard variograms fitted for sorghum yields: anisotropy in four directions (a), isotropic variogram model (model = exponential, nugget = 0, sill = 52,618 kg^2, range = 97,039 m) fitted using weighted least squares (WLS) and its confidence bands (envelopes) (b).

bands show the variability of the sample variogram estimated using simulations from the given set of model parameters, that is, model = exponential, nugget = 0, sill = 52,618 kg^2, and range = 97,039 m. Therefore, isotropic models are used to predict the sorghum yields in Burkina Faso.

In the case of OK interpolation of sorghum yields, the parameters of the exponential variogram show that the average distance up to which the variogram increases is 97 km (Figure 6a). This distance covers approximately 6–10 neighboring terroirs. The variograms of MLR and GWR residuals (Figures 6b–d) show a decrease in both the total sill and range estimates. For RK, this indicates that more variability is taken into the trend component, leaving less for spatial autocorrelation of residuals. For instance, a lower sill of the variogram of GWR residuals shows the strength of the GWR trend, which results in a comparatively low smoothing effect in the sorghum yield map from GWRK as compared to OK (Figure 9). Again the variogram of GWR residuals exhibits a clear spatial structure (Figure 6c). The variogram distance increases up to approximately 18 km. Figure 9d shows the GWRK map of sorghum crop yield, obtained from combining the GWR trend and the predicted GWR residuals.

The results of cross validation (Table 3) show that GWRK performs better than both OK, RK, and KEDLN with an ME value close to 0 (−1.61) and an MSNE value close to 1 (0.869). For all the three kriging methods, the *z*-score values of cross validation show that the variogram models reasonably account for the spatial autocorrelation to explain the yield variance. The RMSE value is lowered for GWRK. No significant spatial structure of the CV residuals is observed. Consequently, the GWRK considerably minimizes the local error variance as compared to OK, KEDLN, and RK (Figures 7a–d and 9d).

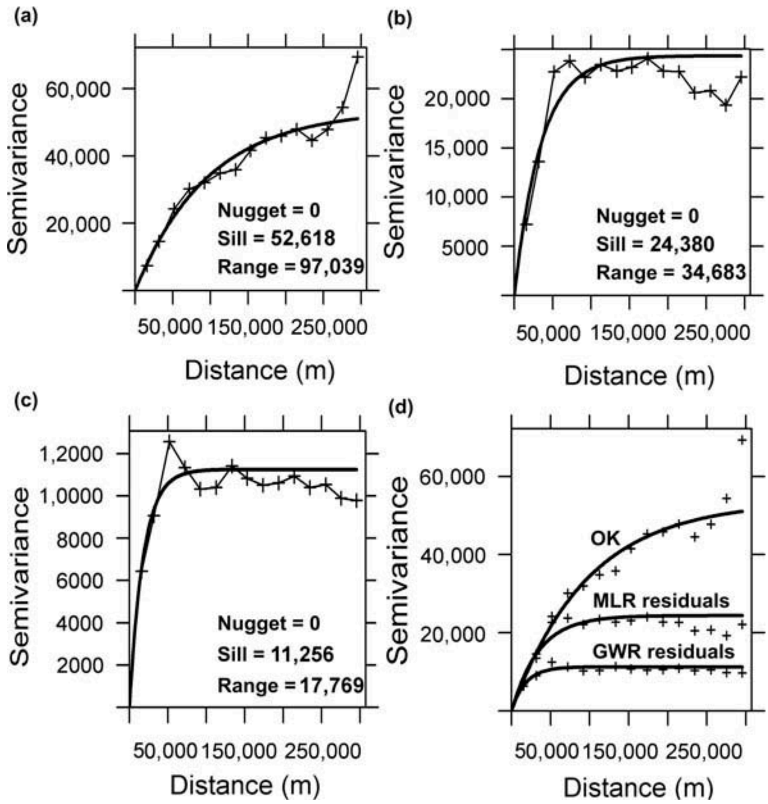

Figure 6. Variograms of ordinary kriging (OK) (a), of residuals of multiple linear regression (MLR) (b) and of residuals of geographically weighted regression (GWR) (c), and their comparison (d).

Table 3. Cross validation (residuals) results of the geostatistical prediction models of sorghum crop yield – ordinary kriging (OK), kriging with external drift using a local kriging neighborhood (KEDLN), regression kriging (RK), and geographically weighted regression kriging (GWRK); for prediction accuracy, we expect mean *z*-score and mean error (ME) close to 0, if the sorghum yield predictions are unbiased, and a small root mean square error (RMSE), if the predictions are close to the measured values. For prediction uncertainty accuracy, we expect the mean square normalized error (MSNE) close to 1, if the standard errors are accurate, the *Z*-score variance is lower than 1, if the kriging variance is not underestimated, and both Moran's I and the correlation (yield predictions and CV residuals) are close to 0, if the CV residuals have no spatial structure.

	Mean	Variance				Moran's I	Correlation
Model	(*Z*-score)	(*Z*-score)	MSNE	ME	RMSE	(CV residuals)	(Yield predictions and CV residuals)
OK	−0.015	0.840	0.701	−3.46	91.2	−0.099	0.126
KEDLN	−0.013	0.804	0.643	−2.12	95	−0.017	0.023
RK	−0.012	0.832	0.687	−3.15	96.4	−0.038	0.218
GWRK	−0.008	0.935	0.869	−1.61	86.9	−0.035	0.025

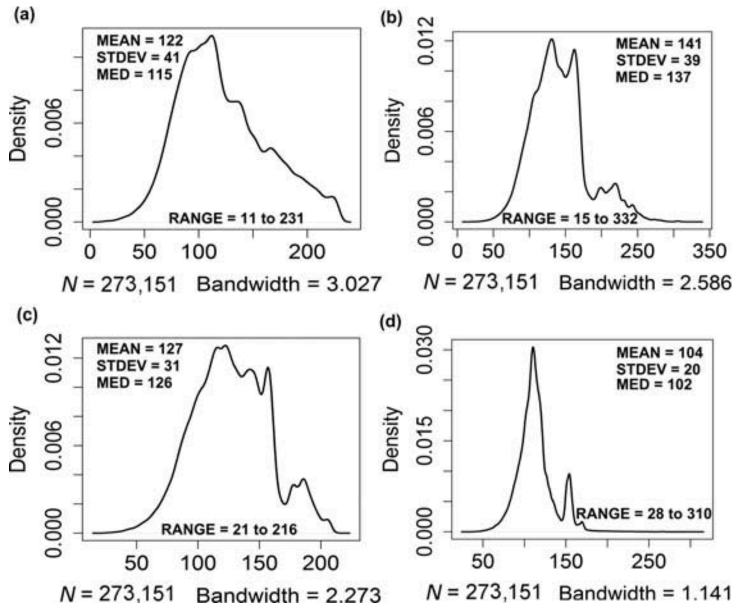

Figure 7. Kernel density plots for local prediction error variances of ordinary kriging (OK) (a), kriging with external drift using a local kriging neighborhood (KEDLN) (b), regression kriging (RK) (c), and geographically weighted regression kriging (GWRK) (d).

3.4. Sorghum yield prediction and uncertainty of prediction

The maps of sorghum crop yield produced by MLR and GWR and the variance of the prediction error are shown in Figure 8. The MLR prediction map presents an overall north–south global trend of sorghum yield. MLR, however, fails to show the short-range spatial variability of sorghum yields, which is clearly present on the Eastern part of maps obtained with geostatistical methods (see Figure 9). The trend identified by MLR shows the strength of external covariates used in the analysis. MLR reduces the prediction variances and tends to make them smooth across the area. For example, MLR overestimates 9.15% of the upper observed sorghum yields and underestimates 8.48% of the lower crop yields. GWR gives 7.76% overfit of the maximum observed yield values. There is a considerable improvement in MAE and MSE values as compared to those values for MLR. The MLR prediction error variance is more uniform over the study area than the GWR.

The summary comparisons of OK, KEDLN, RK, and GWRK (see Table 4) give 4.19% lower mean for OK, and 0.1% lower mean for GWRK, compared to the mean sorghum yield at primary locations. Comparison of sorghum yield maps (Figure 9) shows higher values of the predicted yield (kg ha^{-1}) toward the southern part of Burkina Faso. This indicates that spatial variability of NDVI, precipitation, and elevation successfully explains the favorable cropping conditions along agroecological gradients and between sites. The maps of OK, KEDLN, and RK prediction errors show high residual variability in the northern and NE areas, with 75% values in the range of 11–237. This can be seen from Figure 1a, showing the observed sorghum data are relatively absent in those areas. GWRK considerably reduces this residual variability to 75% values in the range of 28–121. This gives evidence that GWRK effectively utilizes information present in the

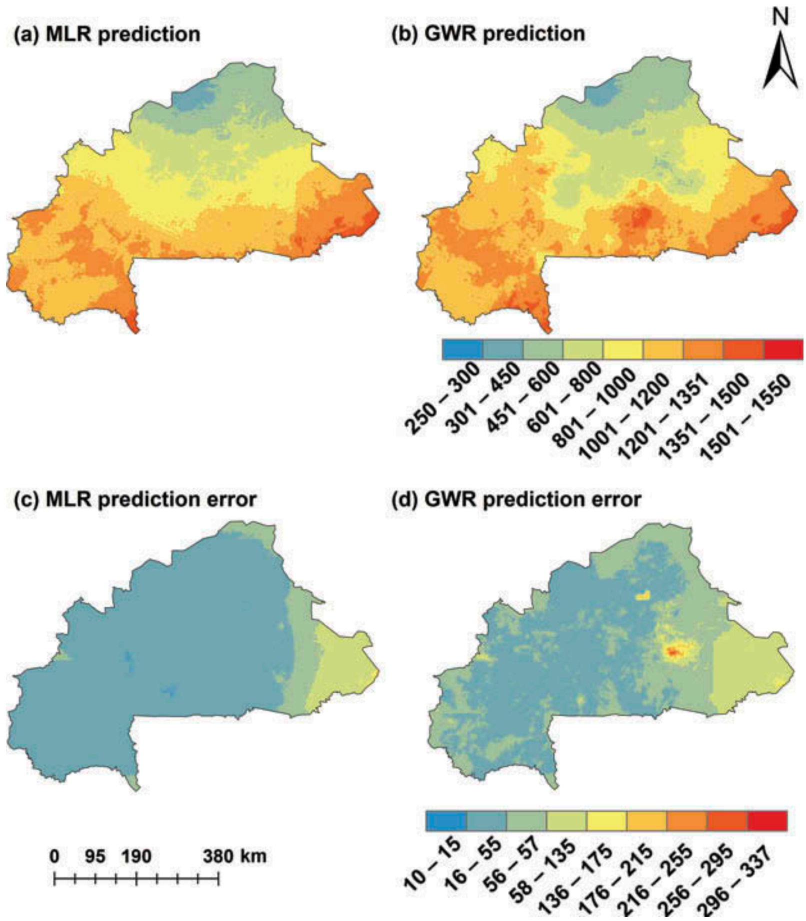

Figure 8. Sorghum crop yield prediction (kg ha^{-1}) from multiple linear regression (MLR) (a), and geographically weighted regression (GWR) (b), estimates of the crop yield prediction uncertainty from MLR (c), and GWR (d).

environmental and management datasets to improve accuracy of the sorghum yield predictions in the study area.

OK interpolation oversmooths the predicted sorghum yields compared to the observed yields. RK improves this smoothing effect, but local error variance is not significantly reduced (see Table 4). Moving from GWR to GWRK improves the prediction (mean) and accuracy of prediction (MAE and MSE). This indicates that the GWR trend fits are not strongly local and captures some of the variation in the data, leaving a relatively low spatial autocorrelation of residuals (Moran's I value of 0.23). Moreover, in GWRK, the prediction error variance is reduced considerably as compared to KEDLN (from 39 to 20) and to RK (from 31 to 20). Moreover, the GWRK predicted mean yield values are accurately estimated as compared to OK, KEDLN, and RK. As compared to KEDLN, the MAE and MSE values are slightly higher in GWRK. Overall, GWRK outperforms all other models both for sorghum yield prediction and in terms of the mean variance of prediction error.

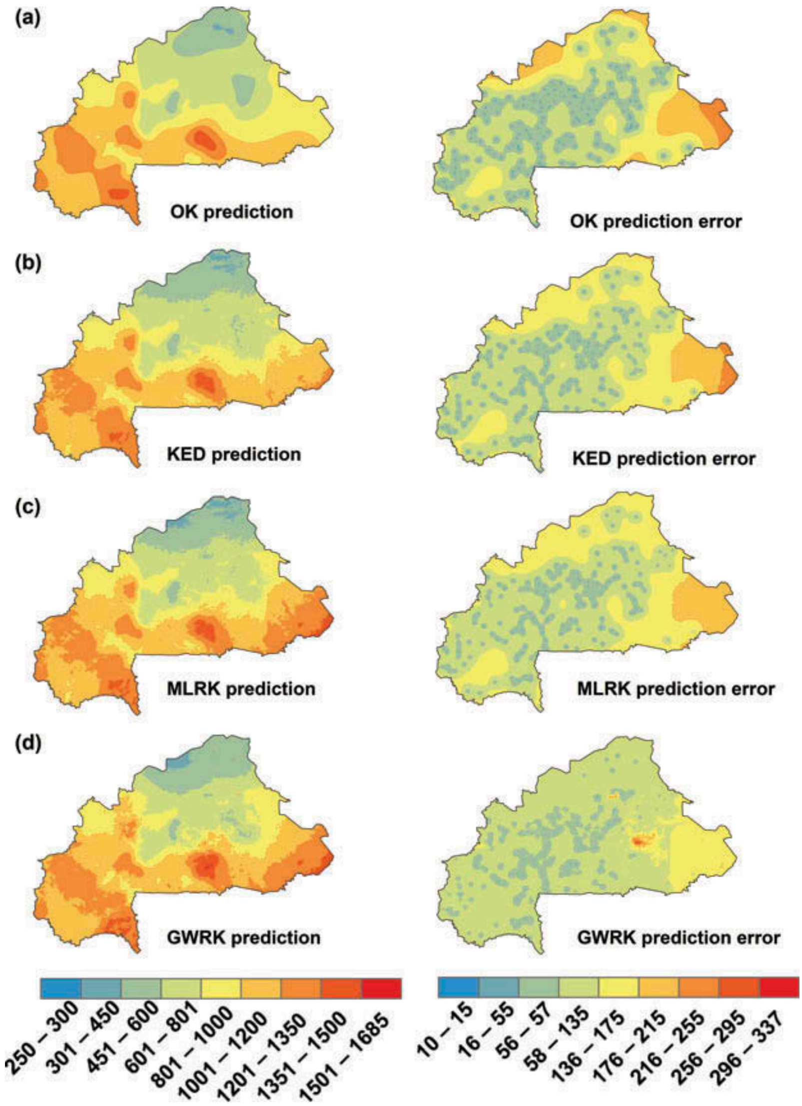

Figure 9. Sorghum crop yield prediction (kg ha^{-1}), and estimates of prediction uncertainty from: ordinary kriging (OK) (a), kriging with external drift using a local kriging neighborhood (KEDLN) (b), regression kriging (RK) (c), and geographically weighted regression kriging (GWRK) (d).

4. Discussion

Kriging (e.g. OK) is a well-established method to model crop within-yield variability for precision agriculture (Faivre *et al.* 2004). There is still a demand for synergistic approaches to accurately model spatial variability of crop yield and its factors over large areas (Challinor *et al.* 2009). Besides producing accurate yield maps, these approaches should produce accurate uncertainty maps for developing wall-to-wall agricultural services. Our focus was therefore on accurately predicting crop yield and associated uncertainties for studies at regional scale. Uncertainties may be associated with field measurements, sampling and monitoring networks, and flaws in the models or in the

Table 4. Histogram descriptive statistics, mean absolute errors (MAE), mean square errors (MSE), and prediction error variance for the sorghum yield predictors – observed sorghum yield (kg ha^{-1}) (training and validation datasets) – models of global multiple linear regression (MLR) and local geographically weighted regression (GWR) – interpolating sorghum yield observations, via ordinary kriging (OK) – predicting sorghum crop yield with external covariate data, via kriging with external drift using a local kriging neighborhood (KEDLN), regression kriging (RK), and geographically weighted regression kriging (GWRK).

Model	n	Min[a]	1st Q[b]	Med[c]	3rd Q	Max[d]	Mean	MAE	MSE	Error variance
Observed (training)	210	421	780	924	1180	1404	954	–	–	–
Observed (validation)	70	421	830	1006	1197	1404	954	–	–	–
MLR	273151	357	787	1004	1135	1531	950	100.0	18426	24
GWR	273151	384	760	1022	1145	1518	958	87.9	11688	27
OK	273151	423	737	934	1071	1417	914	49.4	5457	41
KEDLN	273151	380	731	960	1099	1454	919	54.6	5915	39
RK	273151	382	745	999	1144	1517	944	62.2	7367	31
GWRK	273151	400	753	1010	1148	1560	953	59.0	6953	20

Notes: [a]Minimum.
[b]Quartile.
[c]Median.
[d]Maximum.

statistical analysis itself. In our case study in Burkina Faso, uncertainties may further be dealt with as a result of inadequacy of models to incorporate the spatial variability in large heterogeneous areas. Thus, this study applied a solid statistical methodology for assessing crop yield uncertainty at the national scale. To do so, it quantified jointly and systematically the uncertainties manifested in different sources. The methodology proceeded as follows:

- First, to test the sampling network of representative terroirs, it applied point pattern analysis to check whether the field measurements were not clustered in the country.
- Second, to quantify uncertainty in crop yield predictions, it presented a hybrid approach of GWRK, applying GWR to model the local drift and kriging to interpolate the GWR residuals.
- Third, to test inadequacies in the model itself, it compared the GWRK performance to quantify uncertainty with RK and KEDLN.

GWRK has the potential to predict crop yields accurately over larger areas and to quantify the prediction uncertainty, using external covariate datasets, specifically in situations of spatial nonstationary relations in Burkina Faso that may not be properly modeled by GWR or RK. The accuracy of GWRK is high, provided that sources of the model uncertainty are properly analyzed. In particular, here we discuss the following:

(1) Regional datasets on RURP, PHCR, and market access were obtained from HarvestChoice (2012). HarvestChoice uses a weighted aggregation to prepare these gridded datasets (1 km spatial resolution) at the scale of sub-Saharan Africa. The remaining datasets were RS-based products obtained from SPOT and TAMSAT. All datasets were clipped to the study area and subsequently were used as covariates of the sorghum yield. Input errors like data measurement

and generalization errors were not considered for the covariates, as there was not enough information available to do so. In the future, these errors should be further considered.

(2) Prediction accuracy in regression-based approaches largely depends upon the accuracy of estimated relationships, in particular the spatially nonstationary relationships that may vary according to the spatial scales of each external covariate on crop yield. It is therefore important to carefully determine (1) the effect of sampling network on the spatial nonstationarity of the relationship and (2) the effect of spatial scale of local relationships on the stability and multicollinearity of GWR coefficients. Point pattern analysis confirmed that the spatial nonstationarity observed in the crop yield relationship was not contributed by the sampling network. Moreover, the effect of different adaptive bandwidths was investigated on local estimation in GWR. An optimal bandwidth determines the extent of the spatial neighborhood, to accurately calibrate each locally weighted regression. There is a well-known trade-off between a small bandwidth that may lead to large SEs, and a large bandwidth that may lead to small SEs (Fotheringham *et al.* 2002). In this study, minimizing AIC was used to find an optimal kernel size for local estimation in GWR (Fotheringham *et al.* (2002), p. 212).

(3) In GWR, Harris *et al.* (2010a) showed that the choice of both kernel type and bandwidth optimization method affects the local sample sizes and thus the prediction uncertainty. Presently, there is no well-established method to quantify the uncertainty induced by improper kernel types or improperly calibrated bandwidths of the kernel and, thus, the resulting local parameter uncertainty in GWR. Harris *et al.* (2010a) accessed such uncertainty by calibrating and competing different kernel types and different optimization methods. These comparisons, however, would soon become rather tedious. Here we compared the prediction uncertainty maps from GWRK to other models and, thus, analyzed the model efficiency based on how much the model minimized the local error variance. Our findings showed that GWRK minimized the local error variance as compared to OK, KEDLN, and RK.

(4) To compare GWRK to the study models, we realize that substantial differences occur in their statistical properties. OK is a spatial and univariate interpolator. MLR is a nonspatial and multivariate interpolator and models stationary relationships. GWR is a spatial and multivariate interpolator and models nonstationary relationships. Both KED with a global kriging neighborhood and RK are spatial and multivariate interpolators and model stationary relationships plus spatial dependence in the residual data. Both KED with a KEDLN and GWRK are spatial and multivariate interpolators and model nonstationary relationships plus spatial dependence in the residual data. Contrary to the GWRK, however, KEDLN suffered from local collinearity in this study, and hence, the use of GWRK was preferred.

(5) In RK, the relationship between the dependent variable and external covariates is assumed to be linear. This allowed us to simply sum the drift prediction error variance and the kriging error variance of the predicted residuals, to obtain the RK prediction error variance. Correlations between GWR and the kriging components of GWRK may be complex, and a simple addition of the two variances might result into a considerable bias in the GWRK prediction error variance. Presently, there is no empirical method to estimate such bias. Harris *et al.* (2010a) applied a pragmatic approximation to estimate the GWRK variance by subtracting sill

> estimate of the residual variogram from the sum of the GWR prediction variance and the residual OK variance. Here, this approximation generated a negative GWRK variance. We therefore applied the additive relationship of predictions from Equation (12) to the GWR prediction variance, which resulted in a significantly reduced (non-negative) GWRK error variance. Prediction error variances however should only be used with caution in this study, and in the future, uncertainties are to be characterized by stochastic simulation methods.

Using GWRK and the external covariate datasets, we interpolate the sorghum crop yield over a regular grid covering the country of Burkina Faso, having grid cell size equal to 1 km^2. We intend to use this crop yield interpolation approach for spatializing a BEFM as a spatial decision support at the scale of Burkina Faso. The system will help farmers to formulate on-farm agricultural policies, which we think can be transferred to extension systems throughout the country. We hypothesize that the developed method is of interest to decision-makers and information specialists in the agricultural domain. Approaches to quantify uncertainties in large-area crop models can help to improve the sources of uncertainty given by the sampling design, the model structure and available covariate datasets, and to increase the confidence of decision-makers by taking into account the accurately estimated prediction uncertainty.

5. Conclusion

This research investigated the use of GWRK, to estimate sorghum crop yields and their associated uncertainties in Burkina Faso. It applied geographically weighted regression (GWR) to model the local drift and kriging to interpolate the GWR residuals. It used various global and regional gridded datasets.

The performance of GWRK is compared with that of kriging with RK and kriging with external drift using a KEDLN. Accuracies were compared both for prediction of the sorghum crop yields and for estimating the uncertainty of those predictions. Accuracy of the crop yield prediction is evaluated using MAE, MSE, and the adjusted coefficient of determination, R_a^2. The accuracy of the uncertainty estimates was evaluated using the prediction error variances and the RMSE obtained during cross validation of the residuals. The results indicated that overall GWRK is superior to KEDLN and RK. The MSE value in GWRK was equal to 6953 as compared to 7367 for RK and 5915 for KEDLN. Prediction uncertainty in GWRK was significantly reduced. Prediction error variance in GWRK was equal to 20 as compared to 31 for RK and 39 for KEDLN. GWRK utilized information from external variables in an effective way, and the accuracy of the sorghum crop yield predictions improved. Results showed that climate, topography, financial ability of farmers and labor availability are significant explanatory variables when predicting sorghum crop yield in Burkina Faso. The GWR analysis showed locally a large spatial variation of the parameter estimates. In summary, the study showed how quantification of uncertainties can be an integral part of yield mapping at the national scale.

References

AGRISTAT, 2010. *Résultats Définitives Campagne (2008-2009), Burkina Faso*. Technical report. Ouagadougou: Statistiques sur l'Agriculture et l'Alimentation du Burkina Faso (AGRISTAT).

Baddeley, A. and Turner, R., 2005. Spatstat: an R package for analyzing spatial point patterns. *Journal of Statistical Software*, 12, 1–42.

Bivand, R., Pebesma, E., and Rubio, V., 2008. *Applied spatial data analysis with R*. Heidelberg: Springer.

Brunsdon, C., Fotheringham, A.S., and Charlton, M.E., 1996. Geographically weighted regression: a method for exploring spatial nonstationarity. *Geographical Analysis*, 28 (4), 281–298.

Castoldi, N., Bechini, L., and Stein, A., 2009. Evaluation of the spatial uncertainty of agro-ecological assessments at the regional scale: the phosphorus indicator in northern Italy. *Ecological Indicators*, 9 (5), 902–912. doi:10.1016/j.ecolind.2008.10.009

Challinor, A.J., *et al*., 2009. Crops and climate change: progress, trends, and challenges in simulating impacts and informing adaptation. *Journal of Experimental Botany*, 60 (10), 2775–2789. doi:10.1093/jxb/erp062

Chambers, J.M. and Hastie, T.J., 1992. *Statistical models in S*. Pacific Grove, CA: Wadsworth & Brooks/Cole.

Chilès, J. and Delfiner, P., 1999. *Geostatistics: modeling spatial uncertainty*. New York: Wiley.

Cressie, N., 1993. *Statistics for spatial data*. New York: Wiley.

de Wit, A., de Bruin, S., and Torfs, P., 2008. Representing uncertainty in continental-scale gridded precipitation fields for agrometeorological modeling. *Journal of Hydrometeorology*, 9, 1172–1190. doi:10.1175/2008JHM899.1

Diggle, P., Moyeed, R.A., and Tawn, J.A., 1998. Model-based geostatistics. *Applied Statistics*, 47, 299–350.

Diggle, P.J. and Ribeiro Jr, P.J., 2007. *Model-based geostatistics*. Springer Series in Statistics. New York: Springer, 288.

Dorigo, W., *et al*., 2007. A review on reflective remote sensing and data assimilation techniques for enhanced agroecosystem modeling. *International Journal of Applied Earth Observation and Geoinformation*, 9, 165–193. doi:10.1016/j.jag.2006.05.003

Faivre, R., *et al*., 2004. Spatialising crop models. *Agronomie*, 24, 205–217. doi:10.1051/agro:2004016

FAO, 1998. *Wetland characterization and classification for sustainable agricultural development*. Technical report. Harare: Food and Agriculture Organization – Regional Office for Africa (RAF).

FEWSNET, 2012. *Western Africa FEWS NET food security outlook*. Technical report. Ouagadougou: Famine Early Warning System Network Burkina Faso (FEWSNET).

Fortanier, F., 2006. *Multinational enterprises, commodity chain partnerships and host country development goals*. Technical report. Utrecht: Expert Centre for Sustainable Business and Development Cooperation (ECSAD).

Fotheringham, A., Brunsdon, C., and Charlton, M., 2002. *Geographically weighted regression: the analysis of spatially varying relationships*. New York: Wiley.

Gao, J., *et al*., 2012. Investigating spatial variation in the relationships between NDVI and environmental factors at multi-scales: a case study of Guizhou Karst Plateau, China. *International Journal of Remote Sensing*, 33 (7), 2112–2129. doi:10.1080/01431161.2011.605811

Graef, F. and Haigis, J., 2001. Spatial and temporal rainfall variability in the Sahel and its effects on farmers management strategies. *Journal of Arid Environments*, 48, 221–231. doi:10.1006/jare.2000.0747

Grimes, D.I.F., Igúzquiza, E.P., and Bonifacio, R., 1999. Optimal areal rainfall estimation using raingauges and satellite data. *Journal of Hydrology*, 222, 93–108. doi:10.1016/S0022-1694(99)00092-X

Harris, P., Charlton, M., and Fotheringham, A., 2010b. Moving window kriging with geographically weighted variograms. *Stochastic Environmental Research and Risk Assessment*, 24, 1193–1209. doi:10.1007/s00477-010-0391-2

Harris, P. and Juggins, S., 2011. Estimating freshwater acidification critical load exceedance data for Great Britain using space-varying relationship models. *Mathematical Geosciences*, 43, 265–292. doi:10.1007/s11004-011-9331-z

Harris, P., *et al*., 2010a. The use of geographically weighted regression for spatial prediction: an evaluation of models using simulated data sets. *Mathematical Geosciences*, 42, 657–680. doi:10.1007/s11004-010-9284-7

HarvestChoice, 2012. *Sub-national Sub-Saharan Africa datasets* [online]. HarvestChoice/International Food Policy Research Institute (IFPRI). Available from: http://harvestchoice.org/products/data [Accessed 20 November. 2012].

Heuvelink, G.B.M. and Pebesma, E.J., 1999. Spatial aggregation and soil process modelling. *Geoderma*, 89 (1–2), 47–65. doi:10.1016/S0016-7061(98)00077-9
Kanevski, M., 2008. *Advanced mapping of environmental data*. New York: Wiley.
Kanevski, M. and Maignan, M., 2004. *Analysis and modelling of spatial environmental data*. Lausanne: EPFL Press.
Leopold, U., *et al*., 2006. Accounting for change of support in spatial accuracy assessment of modelled soil mineral phosphorous concentration. *Geoderma*, 130 (3–4), 368–386. doi:10.1016/j.geoderma.2005.02.008
Leung, Y., Mei, C., and Zhang, W., 2000. Statistical tests for spatial nonstationarity based on the geographically weighted regression model. *Environment and Planning A*, 32, 9–32. doi:10.1068/a3162
Lloyd, C.D., 2011. Nonstationary models for exploring and mapping monthly precipitation in the United Kingdom. *International Journal of Climatology*, 30, 390–405.
Maunder, A., 2002. Sorghum worldwide. *In*: J.F. Leslie, ed. *Sorghum and millet diseases*. Ames, IA: Iowa State Press, 11–17.
Papritz, A. and Stein, A., 1999. Spatial prediction by linear kriging. *In*: A. Stein, F. van der Meer, and B. Gorte, eds. *Spatial statistics for remote sensing*. Dordrecht: Kluwer Academic publishers, 83–113.
Pebesma, E.J., 2004. Multivariable geostatistics in S: the gstat package. *Computers & Geosciences*, 30 (7), 683–691. doi:10.1016/j.cageo.2004.03.012
Pebesma, E.J. and Wesseling, C.G., 1998. Gstat: a program for geostatistical modelling, prediction and simulation. *Computers & Geosciences*, 24 (1), 17–31. doi:10.1016/S0098-3004(97)00082-4
Ramankutty, N., 2004. Croplands in West Africa: a geographically explicit dataset for use in models. *Earth Interactions*, 8, 1–22. doi:10.1175/1087-3562(2004)8<1:CIWAAG>2.0.CO;2
Reidsma, P., *et al*., 2009. Regional crop modelling in Europe: the impact of climatic conditions and farm characteristics on maize yields. *Agricultural Systems*, 100 (1–3), 51–60. doi:10.1016/j.agsy.2008.12.009
Reidsma, P., Ewert, F., and Lansink, A.O., 2007. Analysis of farm performance in Europe under different climatic and management conditions to improve understanding of adaptive capacity. *Climatic Change*, 84, 403–422. doi:10.1007/s10584-007-9242-7
Ripley, B.D., 1988. *Statistical inference for spatial processes*. Cambridge University Press.
Rivoirard, J., 2002. On the structural link between variables in kriging with external drift. *Mathematical Geology*, 34, 797–808. doi:10.1023/A:1020972510120
UNCCD, 2000. *Burkina Faso: programme d'action national de lutte contre la désertification*. Technical report. Ouagadougou: United Nations Convention to Combat Desertification (UNCCD).
USGS, 2012. *Hydro Africa datasets (HYDRO1k) of Earth Resource Observation and Science Center (EROS)* [online]. United States Department of the Interior Geological Survey (USGS). Available from: http://eros.usgs.gov/ [Accessed 20 November 2012].
van Ittersum, M.K., *et al*., 2008. Integrated assessment of agricultural systems - A component-based framework for the European Union (SEAMLESS). *Agricultural Systems*, 96 (1–3), 150–165. doi:10.1016/j.agsy.2007.07.009
Vossen, P., 1999. Finding and using data for small scale applications of agrometeorological models such as yield forecasting at a European scale. *In*: A. Stein and F.W.T. Penning de Vries, eds. *Data and models in action*. Dordrecht: Springer, vol. 5, 49–64. doi:10.1007/978-94-015-9217-8_3
West, C.T., Roncoli, C., and Ouattara, F., 2008. Local perceptions and regional climate trends on the Central Plateau of Burkina Faso. *Land Degradation & Development*, 19 (3), 289–304. doi:10.1002/ldr.842
Wheeler, D., 2007. Diagnostic tools and a remedial method for collinearity in geographically weighted regression. *Environment & Planning A*, 39, 2464–2481. doi:10.1068/a38325
Wheeler, D. and Tiefelsdorf, M., 2005. Multicollinearity and correlation among local regression coefficients in geographically weighted regression. *Journal of Geographical Systems*, 7, 161–187. doi:10.1007/s10109-005-0155-6